Hasegawa Y, Kurihara T, Oikawa S, Kinugawa S, Tsutsui H.					
Matsusaka H, Ide T, Matsushima S, Ikeuchi M, Kubota T, Sunagawa K, Kinugawa S, Tsutsui H.	Targeted deletion of p53 prevents cardiac rupture after myocardial infarction in mice	Cardiovasc Res	70	457-65	2006
Matsusaka H, Ide T, Matsushima S, Ikeuchi M, Kubota T, Sunagawa K, Kinugawa S, Tsutsui H	Targeted deletion of matrix metalloproteinase 2 ameliorates myocardial remodeling in mice with chronic pressure overload.	Hypertension	47	711-7	2006
Tomoko MATSUMOTO, Ryuji KOHNO	Performance of Super-Orthogonal Convolutional Coding for Ultra-Wideband Systems in Multipath and Multiuser Channels	Wireless Personal Communications Journal, Kluwer Academic Publishers			2006
Hiroki HARADA, Ryuji KOHNO	Interference Reduction Using a Novel Pulse Set for UWB-CDMA Systems	IEICE TRANS.FUNDAMENTALS	89	3050-58	2006
谷口 健太郎，河野 隆二	TDOA 型センサネットワークにおける階層型粒子フィルタを用いた位置推定法	電子情報通信学会論文誌 A	89-	1068-78	2006
M. Togo, A. Takamura, T. Asai, H. Kaji, M.Nishizawa	An enzyme-based microfluidic biofuel cell using vitamin k3-mediated glucose oxidation	Electrochimica Acta		In press	2007
水野 敏秀，西中 知博，片桐 伸将，佐藤 正喜，田中 秀典，柏原 進，酒井 一成，	ナノサーフェーステクノロジーによる新規生体適合性表面処理 TOYOBO-NCVC コーティングの開発と補助人工心臓および膜型人工肺への応	分子心血管病	7	375-381	2006

松田　智昌，築谷　朋典，本間　章彦，巽　英介，妙中　義之	用.				
Enosawa S, Miyashita T, Saito T, Omasa T, Matsumura T.	The significant improvement of survival times and pathological parameters by bioartificial liver with recominant HepG2 in porcine liver failure model.	Cell Transplantation	15	873-880	2006
Takahashi M, Sakurai M, Enosawa S, Omasa T, Tsuruoka S, Matsumra T.	Double-compartment cell culture apparatus: construction and biochemical evaluation for bioartificial liver support.	Cell Transplantation	15	945-952	2006
大政健史	「工業動物細胞」のゲノム解析　10g/l へ向けたチャレンジ	化学と生物	45	9-11	2007
Abe-Dohmae S, Ueda K, Yokoyama S.	ABCA7, a molecule with unknown function	FEBS Lett.	580	1178-82.	2006
Abe-Dohmae S, Kato KH, Kumon Y, Hu W, Ishigami H, Iwamoto N, Okazaki M, Wu CA, Tsujita M, Ueda K, Yokoyama S.	Serum amyloid A generates high density lipoprotein with cellular lipid in an ABCA1- or ABCA7-dependent manner.	J Lipid Res.	47	1542-50	2006
Kobayashi A, Takanezawa Y, Hirata T, Shimizu Y, Misasa K, Kioka N, Arai H, Ueda K, Matsuo M.	Efflux of sphingomyelin, cholesterol, and phosphatidylcholine by ABCG1.	J Lipid Res.	47	1791-802	2006
Matsumura Y, Ban N, Ueda K, Inagaki N.	Characterization and classification of ATP-binding cassette transporter ABCA3 mutants in fatal surfactant deficiency.	J Biol Chem.	281	34503-14	2006
Mutoh K, Mitsuhashi J, Kimura Y, Tsukahara S, Ishikawa E, Sai K, Ozawa S, Sawada J, Ueda K, Katayama K, Sugimoto Y.	A T3587G germ-line mutation of the MDR1 gene encodes a nonfunctional P-glycoprotein.	Mol Cancer Ther.	5	877-84	2006
Nagao S, Murao K, Imachi H, Cao WM, Yu X, Li J, Matsumoto K, Nishiuchi T, Ahmed RA, Wong NC, Ueda K, Ishida T.	Platelet derived growth factor regulates ABCA1 expression in vascular smooth muscle cells.	FEBS Lett.	580	4371-6	2006
Takahashi K, Kimura Y, Kioka N, Matsuo	Purification and ATPase activity of	J Biol Chem.	281	10760-8	2006

M, Ueda K.	human ABCA1.				
Yazaki K, Yamanaka N, Masuno T, Konagai S, Shitan N, Kaneko S, Ueda K, Sato F.	Heterologous expression of a mammalian ABC transporter in plant and its application to phytoremediation.	Plant Mol Biol.	61	491-503	2006
Kimura Y, Kioka N, Kato H, Matsuo M, Ueda K.	Modulation of drug-stimulated ATPase activity of human MDR1/P-glycoprotein by cholesterol.	Biochem J.	401	597-605	2007
Muto S, Tsuruoka S, Miyata Y, Fujimura A, Asano Y, Kusano E.	Effect of trimethoprim-sulfamethoxazole on Na+ and K+ transport in the rabbit cortical collecting duct.	Nephron Physiol	102	51-60	2006
Sugimoto KI, Araki N, Ohmori M, Harada KI, Cui Y, Tsuruoka S, Kawaguchi A, Fujimura A.	Interaction between grapefruit juice and hypnotic drugs: comparison of triazolam and quazepam.	Eur J Clin Pharmacol.	62	209-215	2006
Yamamoto H, Tsuruoka S, Ioka T, Ando H, Ito C, Akimoto T, Fujimura A, Asano Y, Kusano E.	Indoxyl sulfate stimulates proliferation of rat vascular smooth muscle cells.	Kidney Int.	69	1780-85	2006
Tsuruoka S, Kawaguchi A, Harada K, Fujimura A.	Favorable effect on postgraduate clinical practice of a drug-interaction exercise for undergraduate students.	Eur J Clin Pharmacol.	62	571-6	2006
Tsuruoka S, Watanabe S, Purkerson JM, Fujimura A, Schwartz GJ.	Endothelin and Nitric Oxide Mediate the Adaptation of the Cortical Collecting Duct to Metabolic Acidosis.	Am J Physiol Renal Physiol	291	F866-73	2006
Takahashi M, Sakurai M, Enosawa S, Endo M, Omasa T, Tsuruoka S, Matsumura T.	A double-compartment cell culture apparatus: its construction and biochemical evaluation for bioartificial liver support system.	Cell Transplantation,	15	945–952	2006
Tsuruoka S, Kitoh Y, Kawaguchi A, Sugimoto KI, Hayasaka T, Saito T, Fujimura A.	Clearance of imidapril, an angiotensin-converting enzyme inhibitor, during hemodialysis in hypertensive renal failure patients: Comparison with quinapril and enalapril.	J Clin Pharmacol		In press	2007
Taniguchi J, Tsuruoka S, Mizuno A, Sato JI, Fujimura A, Suzuki M.	TRPV4 as a flow sensor in the flow-dependent K+ secretion from the cortical collecting duct.	Am J Physiol Renal Physiol.		In press	2007
Tsuruoka S, Kaneda T, Ioka T, Fujimura A.	Dosing time-dependent variation of bone resorption by cyclosporin A in rats femurs.	Eur J Pharmacol.		In press	2007
K. Taniguchi, K. Nomura, Y. Hata, T. Nishimura, Y. Asami,	The Si-tag for Immobilizing Proteins on a Silica Surface	Biotechnology and Bioengineering		in press	2007

A. Kuroda					
K. Motomura, N. Takiguchi, H. Ohtake, A. Kuroda	Polyamines affect polyphosphate accumulation in Echerichia coli	J. Environ. Biotech	6	41-46	2006
K Nomura, J. Kato, N. Takiguchi, H. Ohtake, A. Kuroda	Inorganic polyphosphate stimulates Lon-mediated proteolysis of nucleoid proteins in Escherichia coli	Cell. Mol. Biol	52	23-29	2006

別刷りは、平成１８年度分のみを添付しております。

Hands-on Book
ハンズオンブック

PWVを知る PWVで診る

脈波伝播速度
Pulse Wave Velocity

編集
宗像正徳
東北労災病院

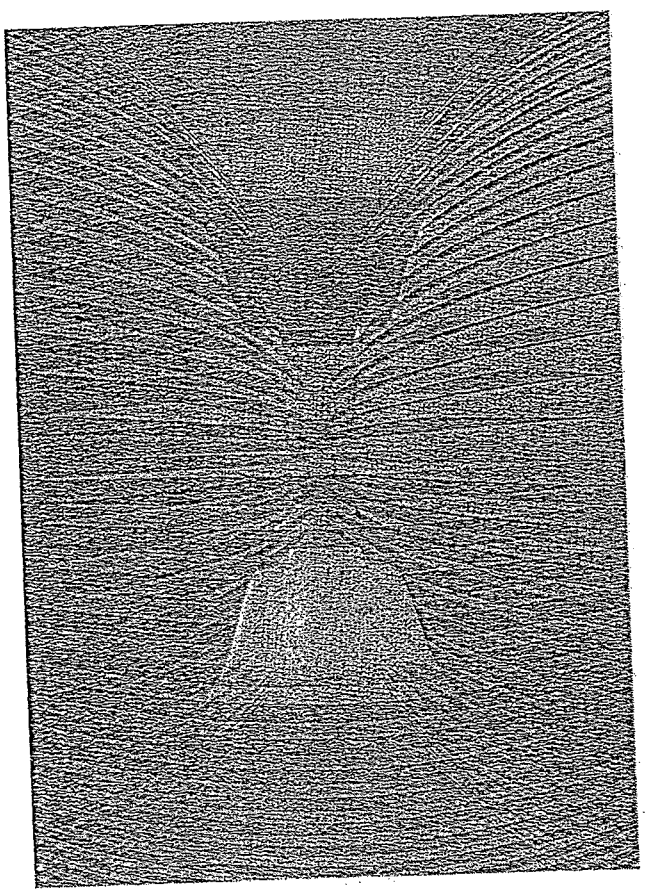

中山書店

2006年8月10日　初版第1刷発行©　〔検印省略〕

Hands-on Book

PWVを知る PWVで診る

編集　宗像正徳
発行者　尾崎仁志
発行所　株式会社 中山書店
〒113-8666　東京都文京区白山1-25-14
TEL 03-3813-1100(代表)　振替 00130-5-196565
http://www.nakayamashoten.co.jp/
DTP　株式会社トライ
印刷・製本　株式会社シナノ
ブックデザイン　藤岡雅史（プロジェクト・エス）

Published by Nakayama-Shoten Co., Ltd.
ISBN 4-521-67651-0 C3347　Printed in Japan

PWVに影響しうる要因とその機序

血圧

PWVはその原理上多くの因子の影響を受ける．そのなかで最も影響が大きいのは年齢，性別，血圧である[1]．血圧のPWVへの影響を考えるとき，慢性的な血圧の影響，すなわち高血圧症による影響と短期的な影響を考える必要がある．高血圧症では，血圧値が高いことに加え動脈の性状自体が変化しているためその解釈も必要である．短期的には刻々と変化する血圧値のため，同じ個体で測定したPWVも変化する．ここでは主に短期的な血圧の影響について述べる．

PWVの原理と血圧値

PWVは動脈の中を進む圧脈波の速度を計測するもので，進んだ距離と要した時間が測定できれば計算できる．すなわち，動脈の中を圧脈波が伝播するとき，その動脈の異なった2点で脈波を記録し，その2点の時間差（ΔT）と2点間の距離（L）を測定すれば，その動脈内を伝播する脈波の速度が計測できる．すなわち，

$$PWV = L/\Delta T$$

で求めることができる．

一方，脈波速度と血管の弾性の関係はMoens-Kortewegの式によれば[2,3]，動脈壁の性状が均一，流速が脈波速度に比べて小さい，圧脈波の振幅が十分に小さく，動脈の長さに比べ半径が十分に小さいとすると，

$$PWV = \sqrt{E \cdot h / 2r \cdot \rho}$$

と表される．ここで，EはYoung率（壁の硬さの指標），hは壁の厚さ，ρは血液の密度である．したがって，壁が硬いほど，壁が厚いほど，半径が小さいほど，血液の密度が小さいほど，PWVは速いことになる（表1）．

ここで，壁の硬さの指標であるYoung率は，物体にある力を加えると，その物体がどれだけ変形する（ひずむ）かを示す物体固有の定数であり（図1），大きいほどその物体は硬いことを表す．動脈はその中に血液が満たされることによって円筒形を保てるぐらいに軟らかいものであるので，動脈壁の硬さは血液の圧力，すなわち血圧値に大きく影響される．よって，同じ血管でも血圧値が

表1 PWV値を大きくする因子

血管壁が硬い
血管壁が厚い
半径が小さい
血液の密度が小さい

Young率

Young率（Young's modulus：弾性率）は，応力に対するひずみの値を決める定数である．
[Young率] ＝ [応力] / [ひずみ]

断面積Sの物体に力Fが加えられ，
元の長さLがΔLだけ変化したとき，

$$E = \frac{F/S}{\Delta L/L}$$

で表される物体の定数EをYoung率（弾性率）という．

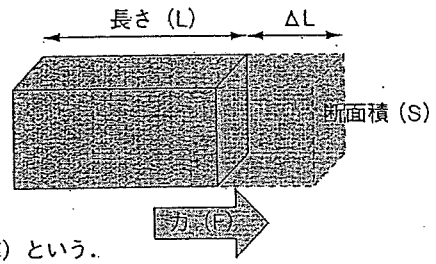

Bergelの補正式

$PWV = \sqrt{E \cdot h / 2r \cdot \rho (1-\sigma^2)}$
σ（Poisson比）＝縦軸 / 横軸 ひずみ

Laplaceの法則

内圧がP，管径がrのとき張力Tは，T＝P×rとなる．
内圧がPのとき，半径rの容器の壁にかかる張力Tを表す．
張力は内圧と管径の積となる．

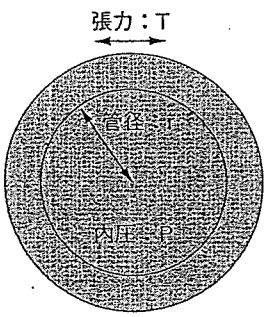

図1 PWVに関する諸式

違えばPWVは大きく変化することになる．

圧脈波による血液密度のひずみを補正するためBergelの補正（図1）をするとより正確ではあるが，圧脈波による血液密度のひずみは小さいため，あまり影響はない．

管内の圧力と壁にかかる張力との関係はLaplaceの法則で示される（図1）．これは，壁にかかる張力は内圧と内径に比例するというものであるので，血圧が上昇すれば血管張力が比例的に増大し，血管が硬くなることを表す．また血管径も増大するためさらに血管壁にかかる張力が増す．

反対に，血圧の上昇による血管径の増大はPWV値を小さくする[4]（図2）．

実際の血圧値とPWV

理想的にいえば，血圧のPWVへの影響を除くには同一血圧で測定して比較すればよい．また多くの健常者で，血圧を変化させながらPWVを計測した特性曲線をプロットし，その平均特性曲線を求め，その曲線との比較により評価する．さらに，この特性曲線は年齢で異なるため各年齢の平均特性曲線を求める．しかし，これらの方法は現実的でない．よって，各年齢で，多くの健常者の1回のみの測定より血圧-PWV平均特性曲線を求め，補正するのが実際的である．健常集団を対象にして収縮期血圧とPWV特性曲線を年代ごとにプロットし，それをもとにして動脈硬化を評価するのが最も妥当であると考えられる．

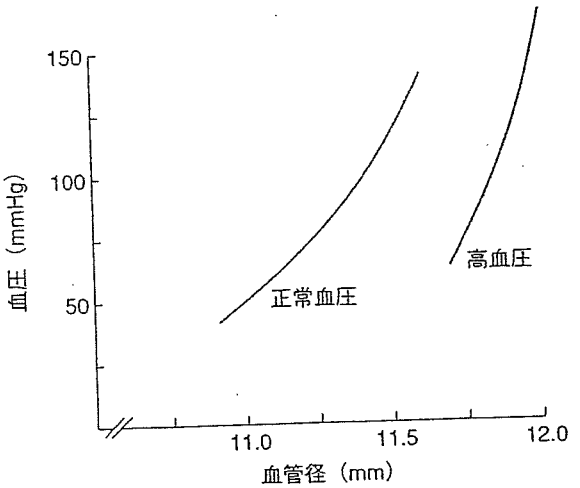

図2 弾性動脈における血管径と血圧の関係
(Nichols WWら，1998[4]より引用)

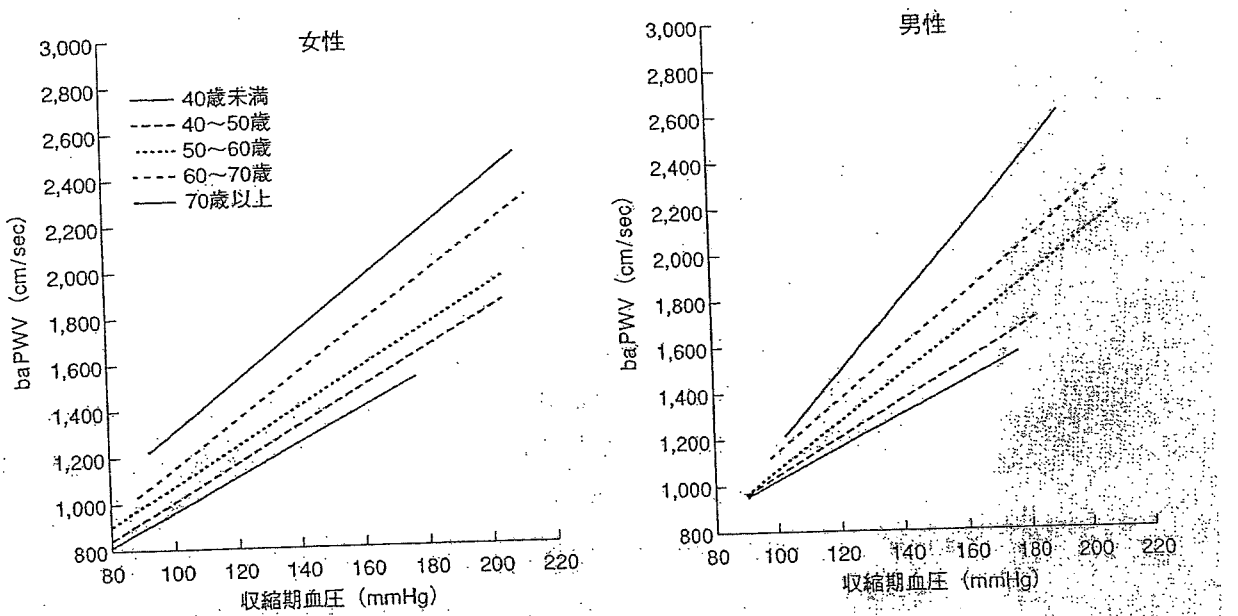

図3 実際の補正式
(東京医科大学，山科章先生の検診データより，コーリンメディカルテクノロジー提供)

PWVと血圧値に関する報告

PWVが血圧値に影響を受けることについては，いくつかの報告があり，いずれも収縮期血圧値とPWVが有意に関連することを報告している．

Asmarらは18～77歳の男女418例で，頸動脈-大腿動脈PWVと年齢，高血圧の関係を示した．正常血圧群も高血圧群もPWVは収縮期血圧および年齢とともに直線的に上昇し，全例でその関係は次式で示された[5]．

PWV(m/sec)＝0.07×収縮期血圧(mmHg)＋0.09×年齢－4.3

Amarらは地域住民993例を対象に，頸動脈-大腿動脈PWVを計測し，心血管

系疾患危険因子との関連を検討した．高脂血症，糖尿病，高血圧に対する未治療群および治療群で年齢，性別，収縮期血圧がPWVと有意に相関した[6]．

Yamashinaらによる血圧値以外の動脈硬化危険因子を有しない日本人での10,000例を超える検討では，多変量解析の結果，baPWV（上腕動脈-足首動脈PWV）に独立して影響を与えるのは年齢，性別，収縮期血圧値であった[1]．

実際の補正

現在広く用いられているform PWV/ABI®（コーリンメディカルテクノロジー）には，東京医科大学山科章先生の検診データをもとにした年齢・性別・血圧での補正式が組み込まれており，年代，血圧値による補正が男女ごとに行われるようになっている[1]（図3）．

血圧補正における問題点と注意点

PWVを血圧値で補正するかどうかについては，議論の余地のあるところである．補正をしないでそのままのPWV値を用いることで，血圧，年齢も含めた動脈硬化の指標として用いるという意見がある一方，血圧値で補正して用いるのが有用という意見もある．

また，血圧-PWV特性曲線は，健常者と動脈硬化のリスクを有する疾患群とでは異なることが考えられるので，この曲線を用いて単純に比較してよいかどうかは不明である．実際，高血圧群では血圧に対する血管径の変化もPWV値の増加も健常群と異なることが報告されている[4,5]．補正式においても，上記で用いられているものは直線的な補正のみであり，補正のやり方を変更すれば，拡張期血圧や脈圧で補正できる可能性もある．

さらに問題となるのが，降圧薬による治療前後でPWVを用いて動脈硬化を評価する場合である．降圧薬は短期的に血圧を変化させるが，血圧の変動を除いても降圧薬の種類によりPWVが変化し，血管壁への効果に差を認めるという報告もある．しかし，降圧薬投与後の特性曲線は投薬前と変化している可能性があり，無投薬時の血圧値で補正することが妥当かどうかは不明である．

今後の展望

現在のところ，血圧値に対する補正は，横断的な報告をもとにした平均的特性曲線を用いて行われているが，今後，縦断的な研究による特性曲線が求められれば，より正確な補正ができると思われる．また，疾患群別の縦断的研究も待たれる．

（山﨑文靖，西永正典，杉浦哲朗，佐藤隆幸）

■文献
1. Yamashina A, et al. Nomogram of the relation of brachial-ankle pulse wave velocity with blood pressure. Hypertens Res 2003；26：801-6.
2. 増田善昭，宮崎　彰．Ⅳ．動脈病変の非観血的診断法　1．中枢および末梢脈波速度．非侵襲的動脈硬化診断研究会編．動脈硬化の診断のガイドライン．東京：共立出版；1999．p.67-75.
3. 入内島十郎．1．脈波の基礎，圧波と血流波：生理学的考察，脈波速度．東京：メジカルビュー社；2002．p.12-6.
4. Nichols WW, O'Rourke MF. McDonald's Blood Flow in Arteries. Theoretical, experimental and clinical principles. 4th ed. London：Arnold；1998. p.379.
5. Asmar R, et al. Assessment of arterial distensibility by automatic pulse wave velocity measurement. Validation and clinical application studies. Hypertension 1995；26：485-90.
6. Amar J, et al. Arterial stiffness and cardiovascular risk factors in a population-based study. J Hypertens 2001；19：381-7.

J Appl Physiol 102: 622–627, 2007.
First published November 2, 2006; doi:10.1152/japplphysiol.00622.2006.

Hypothermia reduces ischemia- and stimulation-induced myocardial interstitial norepinephrine and acetylcholine releases

Toru Kawada,[1] Hirotoshi Kitagawa,[2] Toji Yamazaki,[2] Tsuyoshi Akiyama,[2] Atsunori Kamiya,[1] Kazunori Uemura,[1] Hidezo Mori,[2] and Masaru Sugimachi[1]

[1]*Department of Cardiovascular Dynamics, Advanced Medical Engineering Center, and*
[2]*Department of Cardiac Physiology, National Cardiovascular Center Research Institute, Osaka, Japan*

Submitted 4 June 2006; accepted in final form 1 November 2006

Kawada T, Kitagawa H, Yamazaki T, Akiyama T, Kamiya A, Uemura K, Mori H, Sugimachi M. Hypothermia reduces ischemia- and stimulation-induced myocardial interstitial norepinephrine and acetylcholine releases. *J Appl Physiol* 102: 622–627, 2007. First published November 2, 2006; doi:10.1152/japplphysiol.00622.2006.—Although hypothermia is one of the most powerful modulators that can reduce ischemic injury, the effects of hypothermia on the function of the cardiac autonomic nerves in vivo are not well understood. We examined the effects of hypothermia on the myocardial interstitial norepinephrine (NE) and ACh releases in response to acute myocardial ischemia and to efferent sympathetic or vagal nerve stimulation in anesthetized cats. We induced acute myocardial ischemia by coronary artery occlusion. Compared with normothermia ($n = 8$), hypothermia at 33°C ($n = 6$) suppressed the ischemia-induced NE release [63 nM (SD 39) vs. 18 nM (SD 25), $P < 0.01$] and ACh release [11.6 nM (SD 7.6) vs. 2.4 nM (SD 1.3), $P < 0.01$] in the ischemic region. Under hypothermia, the coronary occlusion increased the ACh level from 0.67 nM (SD 0.44) to 6.0 nM (SD 6.0) ($P < 0.05$) and decreased the NE level from 0.63 nM (SD 0.19) to 0.40 nM (SD 0.25) ($P < 0.05$) in the nonischemic region. Hypothermia attenuated the nerve stimulation-induced NE release from 1.05 nM (SD 0.85) to 0.73 nM (SD 0.73) ($P < 0.05$, $n = 6$) and ACh release from 10.2 nM (SD 5.1) to 7.1 nM (SD 3.4) ($P < 0.05$, $n = 5$). In conclusion, hypothermia attenuated the ischemia-induced NE and ACh releases in the ischemic region. Moreover, hypothermia also attenuated the nerve stimulation-induced NE and ACh releases. The Bezold-Jarisch reflex evoked by the left anterior descending coronary artery occlusion, however, did not appear to be affected under hypothermia.

vagal nerve; sympathetic nerve; cardiac microdialysis; cats

HYPOTHERMIA IS ONE OF THE most powerful modulators that can reduce ischemic injury in the central nervous system, heart, and other organs. The general consensus is that hypothermia induces a hypometabolic state in tissues and balances energy supply and demand (25). With respect to the myocardial ischemia, the size of a myocardial infarction correlates with temperature (6), and mild hypothermia can protect the myocardium against acute ischemic injury (9). The effects of hypothermia on the function of the cardiac autonomic nerves in terms of neurotransmitter releases, however, are not fully understood. Because autonomic neurotransmitters such as norepinephrine (NE) and ACh directly impinge on the myocardium, they would be implicated in the cardioprotection by hypothermia.

In previous studies from our laboratory, Kitagawa et al. (16) demonstrated that hypothermia attenuated the nonexocytotic NE release induced pharmacologically by ouabain, tyramine, or cyanide. Kitagawa et al. (15) also demonstrated that hypothermia attenuated the exocytotic NE release in response to vena cava occlusion or to local administration of high K^+. The effects of hypothermia on the ischemia-induced myocardial interstitial NE release, however, were not examined in those studies. In addition, the effects of hypothermia on the ischemia-induced myocardial interstitial ACh release have never been examined. Because both sympathetic and parasympathetic nerves control the heart, simultaneous monitoring of the myocardial interstitial releases of NE and ACh (14, 31) would help integrative understanding of the autonomic nerve terminal function under hypothermia in conjunction with acute myocardial ischemia.

In the present study, the effects of hypothermia on the ischemia-induced and nerve stimulation-induced myocardial interstitial neurotransmitter releases were examined. We implanted a dialysis probe into the left ventricular free wall of anesthetized cats and measured dialysate NE and ACh levels as indexes of neurotransmitter outputs from the cardiac sympathetic and vagal nerve terminals, respectively. Based on our laboratory's previous results (15, 16), we hypothesized that hypothermia would attenuate the neurotransmitter releases in response to acute myocardial ischemia and to electrical nerve stimulation.

MATERIALS AND METHODS

Surgical Preparation and Protocols

Animals were cared for in accordance with the *Guiding Principles for the Care and Use of Animals in the Field of Physiological Sciences*, approved by the Physiological Society of Japan. All protocols were reviewed and approved by the Animal Subjects Committee of National Cardiovascular Center. Adult cats were anesthetized via an intraperitoneal injection of pentobarbital sodium (30–35 mg/kg) and ventilated mechanically through an endotracheal tube with oxygen-enriched room air. The level of anesthesia was maintained with a continuous intravenous infusion of pentobarbital sodium (1–2 $mg \cdot kg^{-1} \cdot h^{-1}$) through a catheter inserted from the right femoral vein. Mean arterial pressure (MAP) was measured using a pressure transducer connected to a catheter inserted from the right femoral artery. Heart rate (HR) was determined from an electrocardiogram.

Protocol 1: acute myocardial ischemia. We examined the effects of hypothermia on the ischemia-induced myocardial interstitial releases of NE and ACh. The heart was exposed by partially removing the left fifth and/or sixth rib. A dialysis probe was implanted transversely into

Address for reprint requests and other correspondence: T. Kawada, Dept. of Cardiovascular Dynamics, Advanced Medical Engineering Center, National Cardiovascular Center Research Institute, 5-7-1 Fujishirodai, Suita, Osaka 565-8565, Japan (e-mail: torukawa@res.ncvc.go.jp).

The costs of publication of this article were defrayed in part by the payment of page charges. The article must therefore be hereby marked "*advertisement*" in accordance with 18 U.S.C. Section 1734 solely to indicate this fact.

the anterolateral free wall of the left ventricle perfused by the left anterior descending coronary artery (LAD) to monitor myocardial interstitial NE and ACh levels in the ischemic region during occlusion of the LAD (13). Another dialysis probe was implanted transversely into the posterior free wall of the left ventricle perfused by the left circumflex coronary artery to monitor myocardial interstitial NE and ACh levels in a nonischemic region. Heparin sodium (100 U/kg) was administered intravenously to prevent blood coagulation. Animals were divided into a normothermic group (n = 8) and a hypothermic group (n = 6). In the hypothermic group, surface cooling with ice bags was performed until the esophageal temperature decreased to 33°C (15, 16). A stable hypothermic condition was obtained within ~2 h. In each group, we occluded the LAD for 60 min and examined changes in the myocardial interstitial NE and ACh levels in the ischemic region (i.e., the LAD region) and nonischemic region (i.e., the left circumflex coronary artery region). Fifteen-minute dialysate samples were obtained during the preocclusion baseline condition and during the periods of 0–15, 15–30, 30–45, and 45–60 min of the LAD occlusion.

Protocol 2: sympathetic stimulation. We examined the effects of hypothermia on the sympathetic nerve stimulation-induced myocardial interstitial NE release (n = 6). A dialysis probe was implanted transversely into the anterolateral free wall of the left ventricle. The bilateral cardiac sympathetic nerves originating from the stellate ganglia were exposed through a second intercostal space and sectioned. The cardiac end of each sectioned nerve was placed on a bipolar platinum electrode for sympathetic stimulation (5 Hz, 10 V, 1-ms pulse duration). The electrodes and nerves were covered with mineral oil to provide insulation and prevent desiccation. A 4-min dialysate sample was obtained during the sympathetic stimulation under the normothermic condition. Thereafter, hypothermia was introduced using the same cooling procedure as in *protocol 1*, and a second 4-min dialysate sample was obtained during the sympathetic stimulation.

Protocol 3: vagal stimulation. We examined the effects of hypothermia on the vagal nerve stimulation-induced ACh release (n = 5). A dialysis probe was implanted transversely into the anterolateral free wall of the left ventricle. The bilateral vagi were exposed through a midline cervical incision and sectioned at the neck. The cardiac end of each sectioned nerve was placed on a bipolar platinum electrode for vagal stimulation (20 Hz, 10 V, 1-ms pulse duration). To prevent severe bradycardia and cardiac arrest, which can be induced by the vagal stimulation, the heart was paced at 200 beats/min using pacing wires attached to the apex of the heart during the stimulation period. A 4-min dialysate sample was obtained during the vagal stimulation under the normothermic condition. Thereafter, hypothermia was introduced using the same cooling procedure as in *protocol 1*, and a second 4-min dialysate sample was obtained during the vagal stimulation.

Because of the relatively intense stimulation of the sympathetic or vagal nerve, the stimulation period in *protocols 2* and *3* was limited to 4 min to minimize gradual waning of the stimulation effects. At the end of the experiment, the animals were killed by increasing the depth of anesthesia with an overdose of pentobarbital sodium. We then confirmed that the dialysis probes had been threaded in the middle layer of the left ventricular myocardium.

Dialysis Technique

The dialysate NE and ACh concentrations were measured as indexes of myocardial interstitial NE and ACh levels, respectively. The materials and properties of the dialysis probe have been described previously (2, 3). Briefly, we designed a transverse dialysis probe. A dialysis fiber (13-mm length, 310-μm outer diameter, 200-μm inner diameter; PAN-1200, 50,000 molecular weight cutoff; Asahi Chemical) was connected at both ends to polyethylene tubes (25-cm length, 500-μm outer diameter, 200-μm inner diameter). The dialysis probe was perfused with Ringer solution containing a cholinesterase inhibitor eserine (10^{-4} M) at a rate of 2 μl/min. We started dialysate sampling from 2 h after the implantation of the dialysis probe(s), when the dialysate NE and ACh concentrations had reached steady states. The actual dialysate sampling was delayed by 5 min from the collection period to account for the dead space volume between the semipermeable membrane and the sample tube. Each sample was collected in a microtube containing 3 μl of HCl to prevent amine oxidation. The dialysate ACh concentration was measured directly by HPLC with electrochemical detection (Eicom). The in vitro recovery rate of ACh was ~70%. With the use of a criterion of signal-to-noise ratio of higher than three, the detection limit for ACh was 3 pg per injection. The dialysate NE concentration was measured by another HPLC-electrochemical detection system after the removal of interfering compounds by an alumina procedure. The in vitro recovery rate of NE was ~55%. With the use of a criterion of signal-to-noise ratio of higher than three, the detection limit for NE was 200 fg per injection.

Statistical Analysis

All data are presented as means and SD values. For *protocol 1*, we performed two-way repeated-measures ANOVA using hypothermia as one factor and the dialysate sampling periods (the effects of ischemia) as the other factor. For *protocols 2* and *3*, we compared stimulation-induced releases of NE and ACh before and during hypothermia using a paired t-test. For all of the statistics, the difference was considered significant when $P < 0.05$.

RESULTS

Figure 1*A* illustrates changes in myocardial interstitial NE levels in the ischemic region during LAD occlusion obtained from *protocol 1*. The *inset* shows the magnified ordinate for the

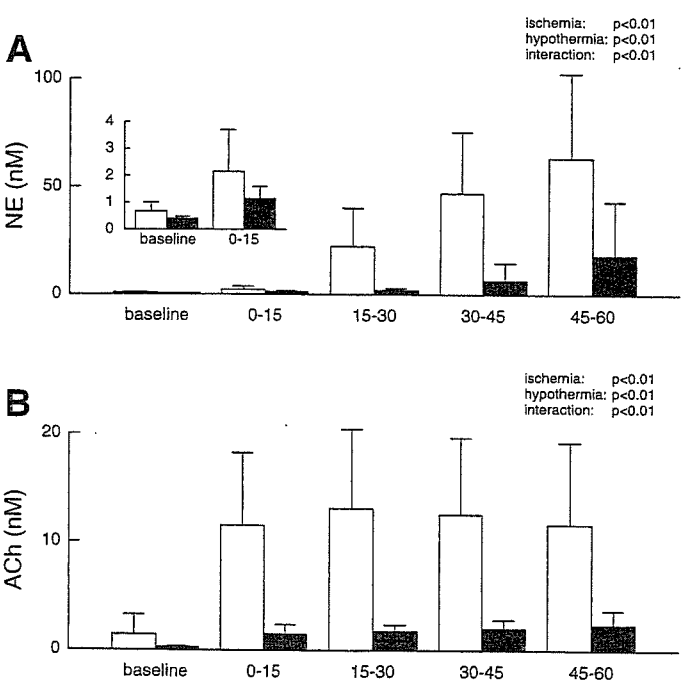

Fig. 1. *A*: ischemia-induced myocardial interstitial norepinephrine (NE) release in the ischemic region. Acute myocardial ischemia caused a progressive increase in the level of myocardial interstitial NE. Hypothermia attenuated the ischemia-induced NE release. *Inset*: magnified ordinate for the baseline and the 0- to 15-min period of ischemia. *B*: ischemia-induced myocardial interstitial ACh release in the ischemic region. Acute myocardial ischemia increased the myocardial interstitial ACh levels. Hypothermia attenuated the ischemia-induced ACh release. Open bars: normothermia; solid bars: hypothermia.

baseline and the 0- to 15-min period of ischemia. In the normothermic group (open bars), the LAD occlusion caused an ~94-fold increase in the NE level during the 45- to 60-min interval. In the hypothermic group (solid bars), the LAD occlusion caused an ~45-fold increase in the NE level during the 45- to 60-min interval. Compared with normothermia, hypothermia suppressed the baseline NE level to ~59% and the NE level during the 45- to 60-min period to ~29%. Statistical analysis indicated that the effects of both hypothermia and ischemia on the NE release were significant, and the interaction between hypothermia and ischemia was also significant.

Figure 1*B* illustrates changes in myocardial interstitial ACh levels in the ischemic region during the LAD occlusion. In both the normothermic (open bars) and hypothermic (solid bars) groups, the LAD occlusion caused an approximately eightfold increase in the ACh level during the 45- to 60-min interval. Compared with normothermia, however, hypothermia suppressed both the baseline ACh level and the ACh level during the 45- to 60-min period of ischemia to ~20%. Statistical analysis indicated that the effects of both hypothermia and ischemia on the ACh release were significant, and the interaction between hypothermia and ischemia was also significant.

Figure 2*A* illustrates changes in myocardial interstitial NE levels in the nonischemic region during the LAD occlusion. Note that scale of the ordinate is only one-hundredth of that in Fig. 1*A*. The LAD occlusion decreased the NE level in the normothermic group (open bars); the NE level during the 45- to 60-min interval was ~59% of the baseline level. The LAD occlusion also decreased the NE level in the hypothermic group (solid bars); the NE level during the 45- to 60-min interval was ~64% of the baseline level. Although the LAD occlusion resulted in a decrease in the NE level under both conditions, the NE level under hypothermia was nearly twice that measured under normothermia. The statistical analysis indicated that the effects of both hypothermia and ischemia on the NE release were significant, whereas the interaction between hypothermia and ischemia was not significant.

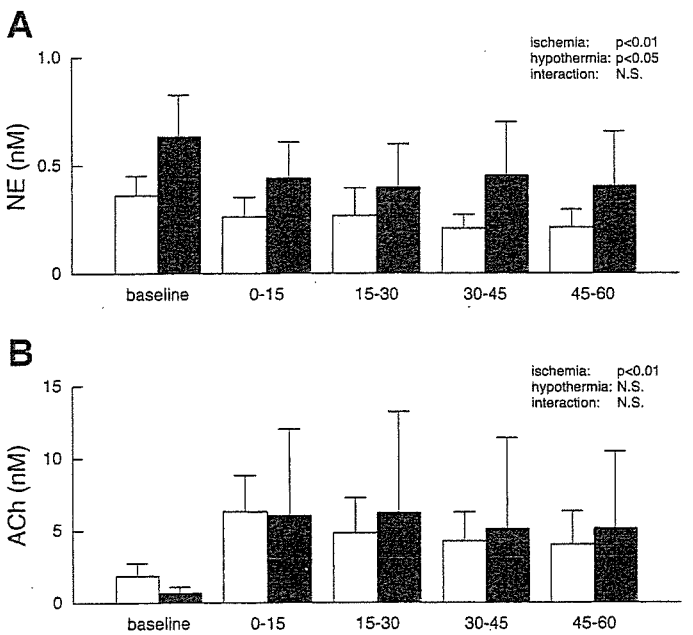

Fig. 2. *A*: changes in the myocardial interstitial NE levels in the nonischemic region. Acute myocardial ischemia decreased the level of myocardial interstitial NE from the baseline level. Hypothermia increased the myocardial interstitial NE levels in the nonischemic region. *B*: changes in the myocardial interstitial ACh levels in the nonischemic region. Acute myocardial ischemia increased the myocardial interstitial ACh level. Hypothermia did not attenuate the increasing response of ACh to the left anterior descending coronary artery occlusion. Open bars: normothermia; solid bars: hypothermia. NS, not significant.

Table 1. *Mean arterial pressure during acute myocardial ischemia obtained in protocol 1*

	Baseline	5 min	15 min	30 min	45 min	60 min
Normothermia	108 (23)	102 (28)	101 (24)	101 (20)	102 (21)	102 (21)
Hypothermia	108 (11)	80 (17)	87 (10)	85 (10)	86 (10)	91 (11)

Values are means (SD) (in mmHg) obtained during preocclusion baseline period and 5-, 15-, 30-, 45-, and 60-min periods of coronary artery occlusion. Ischemia: $P < 0.01$; hypothermia: not significant; interaction: $P < 0.01$.

Figure 2*B* illustrates changes in myocardial interstitial ACh levels in the nonischemic region during the LAD occlusion. The LAD occlusion caused an ~3.4-fold increase in the ACh level during the 0- to 15-min interval in the normothermic group (open bars). The LAD occlusion caused an approximately ninefold increase in the ACh level during the 0- to 15-min interval in the hypothermic group (solid bars). These effects of ischemia on the ACh release were statistically significant. Although hypothermia seemed to attenuate the baseline ACh level, the overall effects of hypothermia on the ACh level were insignificant.

Tables 1 and 2 summarize the MAP and HR data, respectively, obtained in *protocol 1*. Acute myocardial ischemia significantly reduced MAP ($P < 0.01$) and HR ($P < 0.01$). Hypothermia did not affect MAP but did decrease HR ($P < 0.01$). The interaction between ischemia and hypothermia was significant for MAP but not for HR by the two-way repeated-measures ANOVA.

For *protocol 2*, hypothermia significantly attenuated the sympathetic stimulation-induced NE release to ~70% of the level observed during normothermia (Fig. 3*A*). Under normothermia, the sympathetic stimulation increased MAP from 114 mmHg (SD 27) to 134 mmHg (SD 33) ($P < 0.01$) and HR from 147 beats/min (SD 9) to 207 beats/min (SD 5) ($P < 0.01$). Under hypothermia, the sympathetic stimulation increased MAP from 117 mmHg (SD 11) to 136 mmHg (SD 22) ($P < 0.05$) and HR from 125 beats/min (SD 16) to 164 beats/min (SD 10) ($P < 0.01$).

For *protocol 3*, hypothermia significantly attenuated the vagal stimulation-induced ACh release to ~70% of the level observed during normothermia (Fig. 3*B*). Hypothermia did not change MAP [117 mmHg (SD 18) vs. 118 mmHg (SD 27)] but

Table 2. *Heart rate during acute myocardial ischemia obtained in protocol 1*

	Baseline	5 min	15 min	30 min	45 min	60 min
Normothermia	183 (26)	160 (18)	163 (16)	163 (18)	166 (20)	165 (21)
Hypothermia	146 (25)	116 (19)	113 (19)	126 (39)	112 (20)	97 (31)

Values are means (SD) (in beats/min) obtained during preocclusion baseline period and 5-, 15-, 30-, 45-, and 60-min periods of coronary artery occlusion. Ischemia: $P < 0.01$; hypothermia: $P < 0.01$; interaction: not significant.

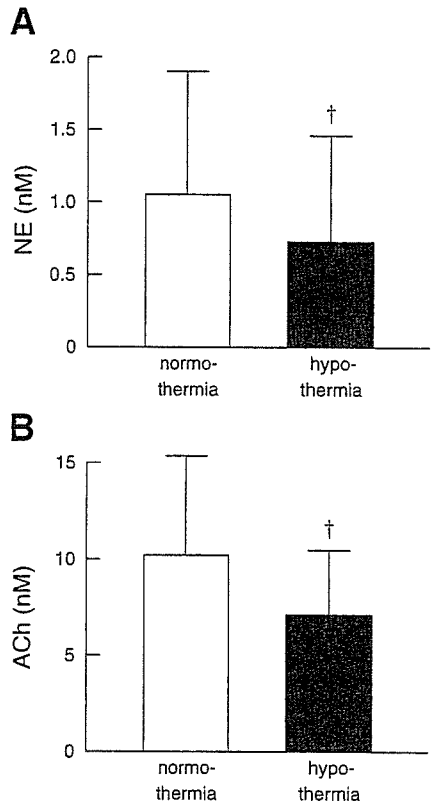

Fig. 3. *A*: efferent sympathetic nerve stimulation-induced release of myocardial interstitial NE before and during hypothermia. †Hypothermia significantly attenuated the stimulation-induced NE release. *B*: efferent vagal nerve stimulation-induced release of myocardial interstitial ACh before and during hypothermia. †Hypothermia significantly attenuated the stimulation-induced ACh release.

did decrease HR from 202 beats/min (SD 24) to 179 beats/min (SD 15) ($P < 0.05$) during the prestimulation, unpaced condition. MAP during the stimulation was 105 mmHg (SD 19) under normothermia and 93 mmHg (SD 33) under hypothermia.

DISCUSSION

A cardiac microdialysis is a powerful tool to estimate neurotransmitter levels in the myocardial interstitium in vivo (2, 3, 14, 19, 20, 31). The present study demonstrated that hypothermia significantly attenuated the myocardial interstitial releases of NE and ACh in the ischemic region during the LAD occlusion. In contrast, the increasing response in the ACh level from its baseline level and the decreasing response in the NE level from its baseline level observed in the nonischemic region were maintained under hypothermia. To our knowledge, this is the first report showing the effects of hypothermia on the myocardial interstitial releases of NE and ACh during acute myocardial ischemia in vivo. In addition, the present study showed that hypothermia significantly attenuated nerve stimulation-induced myocardial interstitial NE and ACh releases in vivo.

Effects of Hypothermia on Ischemia-induced NE and ACh Releases in the Ischemic Region

Acute myocardial ischemia causes energy depletion, which leads to myocardial interstitial NE release in the ischemic region (Fig. 1*A*). The NE release can be classified as exocytotic or nonexocytotic (18, 24). Exocytotic release indicates NE release from synaptic vesicles, which normally occurs in response to nerve discharge and subsequent Ca^{2+} influx through voltage-dependent Ca^{2+} channels. On the other hand, nonexocytotic release indicates NE release from the axoplasm, such as that mediated by a reverse transport through the NE transporter. A neuronal uptake blocker, desipramine, can suppress the ischemia-induced NE release (19, 24). Whereas exocytotic release contributes to the ischemia-induced NE release in the initial phase of ischemia (within ~20 min), carrier-mediated nonexocytotic release becomes predominant as the ischemic period is prolonged (1). Hypothermia significantly attenuated the ischemia-induced NE release (Fig. 1*A*). The NE level during the 45- to 60-min period of ischemia under hypothermia was ~20% of that obtained under normothermia. The NE uptake transporter is driven by the Na^+ gradient across the cell membrane (23). The loss of the Na^+ gradient due to ischemia causes NE to be transported out of the cell by reversing the action of the NE transporter. Hypothermia inhibits the action of the NE transporter and also suppresses the intracellular Na^+ accumulation (8), thereby reducing nonexocytotic NE release during ischemia. The present results are in line with an in vitro study that showed hypothermia suppressed nonexocytotic NE release induced by deprivation of oxygen and glucose (30). The present results are also consistent with a previous study from our laboratory that showed hypothermia attenuated the nonexocytotic NE release induced by ouabain, tyramine, or cyanide (16).

Acute myocardial ischemia increases myocardial interstitial ACh level in the ischemic region, as reported previously (Fig. 1*B*) (13). The level of ischemia-induced ACh release during 0- to 15-, 15- to 30-, 30- to 45-, or 45- to 60-min period of ischemia is comparable to that evoked by 4-min electrical stimulation of the bilateral vagi (Fig. 3*B*). Compared with the normothermic condition, hypothermia significantly attenuated the ischemia-induced myocardial interstitial release of ACh in the ischemic region. Our laboratory's previous study indicated that intracellular Ca^{2+} mobilization is essential for the ischemia-induced release of ACh (13). Hypothermia may have prevented the Ca^{2+} overload, thereby reducing the ischemia-induced ACh release. Alternatively, hypothermia may reduce the extent of the ischemic injury, which in turn suppressed the ischemia-induced ACh release. Because ACh has protective effects on the cardiomyocytes against ischemia (11), the suppression of ischemia-induced ACh release during hypothermia itself may be unfavorable for cardioprotection.

There is considerable controversy regarding the cardioprotective effects of β-adrenergic blockade during severe ischemia, with studies demonstrating a reduction of infarct size (10, 17) or no effects (7, 27). The β-adrenergic blockade seems effective to protect the heart only when the heart is reperfused within a certain period after the coronary occlusion. The β-adrenergic blockade would reduce the myocardial oxygen consumption through the reduction of HR and ventricular contractility and delay the progression of ischemic injury. Hence the infarct size might be reduced when the heart is reperfused before the ischemic damage becomes irreversible. The ischemia-induced NE release reached nearly 100 times the baseline NE level under normothermia (Fig. 1*A*), which by far exceeded the NE level attained by electrical stimulation of the

bilateral stellate ganglia (Fig. 3*A*). Because high NE levels have cardiotoxic effects (22), ischemia-induced NE release might aggravate the ischemic injury. However, catecholamine depletion by a reserpine treatment fails to reduce the infarct size (26, 29), throwing a doubt on the involvement of catecholamine toxicity in the progression of myocardial damage during ischemia. It is, therefore, most likely that the hypothermia-induced reductions in NE and ACh are the result of reduced myocardial damage or a direct effect on nerve endings.

Van den Doel et al. (28) showed that hypothermia does not abolish necrosis, but rather delays necrosis during sustained ischemia, so that hypothermia protected against infarction produced by a 30-min occlusion but not against infarction produced by a 60-min occlusion in the rat heart. At the same time, they mentioned that hypothermia was able to reduce the infarct size after a 60-min coronary occlusion in the dog, possibly because of the significant collateral flow in the canine hearts. Because the feline hearts are similar to the canine hearts in that they have considerable collateral flow compared with the rat hearts (21), hypothermia should have protected the feline heart against the 60-min coronary occlusion in the present study.

Effects of Hypothermia on the NE and ACh Releases in the Nonischemic Region and on the Electrical Stimulation-induced NE and ACh Releases

The NE and ACh levels in the nonischemic region may reflect the sympathetic and parasympathetic drives to this region. As an example, myocardial interstitial ACh levels increase during activations of the arterial baroreflex and the Bezold-Jarisch reflex (14). In the present study, acute myocardial ischemia decreased the NE level from its baseline level, whereas it increased the ACh level from its baseline level (Fig. 2). Ischemia also decreased MAP and HR (Tables 1 and 2), suggesting that the Bezold-Jarisch reflex was induced by the LAD occlusion under both normothermia and hypothermia. Taking into account the fact that electrical stimulation-induced ACh release was attenuated to ~70% (Fig. 3), similar ACh levels during ischemia imply the enhancement of the parasympathetic outflow via the Bezold-Jarisch reflex under hypothermia. These results are in line with the study by Zheng et al. (32), where pulmonary chemoreflex-induced bradycardia was maintained under hypothermia. Hypothermia increased the NE level in the nonischemic region, suggesting that sympathetic drive to this region also increased. Hypothermic stress is known to cause sympathetic activation, accompanying increases in MAP, HR, plasma NE, and epinephrine levels (4). In the present study, because the effect of hypothermia on MAP was insignificant (Table 1) and HR decreased under hypothermia (Table 2), the sympathetic activation observed in the nonischemic region might have been regional and not systemic.

Hypothermia attenuated the releases of NE and ACh in response to respective nerve stimulation to ~70% of that observed under normothermia (Fig. 3). The suppression of the exocytotic NE release by hypothermia is consistent with a previous study from our laboratory, where hypothermia attenuated the myocardial interstitial NE release in response to vena cava occlusion or to a local high K^+ administration (15). The suppression of NE release by hypothermia is consistent with an in vitro study by Kao and Westhead (12) in which catecholamine secretion from adrenal chromaffin cells induced by elevated K^+ levels increased as the temperature increased from 4 to 37°C. On the other hand, because hypothermia inhibits the neuronal NE uptake, the NE concentration at the synaptic cleft is expected to be increased if the level of NE release remains unchanged. Actually, Vizi (30) demonstrated that hypothermia increased NE release in response to field stimulation in vitro. In the present study, however, the suppression of NE release might have canceled the potential accumulation of NE due to NE uptake inhibition. The present study also demonstrated that the ACh release was suppressed by hypothermia. In the rat striatum, hypothermia decreases the extracellular ACh concentration and increases the choline concentration (5). Hypothermia may inhibit a choline uptake transporter in the same manner as it inhibits a NE uptake transporter. The inhibition of the choline transporter by hypothermia may have hampered the replenishment of the available pool of ACh and thereby contributed to the suppression of the stimulation-induced ACh release.

Limitations

In *protocol 1*, because we did not measure the infarct size in the present study, the degree of myocardial protection by hypothermia was undetermined. Whether the reduction of ischemia-induced neurotransmitter release correlates with the reduction of infact size requires further investigations. In *protocols 2* and *3*, baseline NE and ACh levels were not measured. The reduction of stimulation-induced NE and ACh release by hypothermia might be partly due to the reduction of baseline NE and ACh levels. However, because transection of the stellate ganglia (31) or vagi (3) reduces the baseline NE and ACh levels, changes in the baseline NE and ACh levels by hypothermia in *protocols 2* and *3* could not be as large as those observed under innervated conditions in *protocol 1* (Figs. 1 and 2).

In conclusion, hypothermia attenuated the ischemia-induced releases of NE and ACh in the ischemic region to ~30 and 20% of those observed under normothermia, respectively. Hypothermia also attenuated the nerve stimulation-induced releases of NE and ACh to ~70% of those observed during normothermia. In contrast, hypothermia did not affect the decreasing response in the NE level and the increasing response in the ACh level in the nonischemic region, suggesting that the Bezold-Jarisch reflex evoked by the LAD occlusion was maintained.

GRANTS

This study was supported by Health and Labour Sciences Research Grant for Research on Advanced Medical Technology, Health and Labour Sciences Research Grant for Research on Medical Devices for Analyzing, Supporting and Substituting the Function of Human Body, and Health and Labour Sciences Research Grant H18-Iryo-Ippan-023 from the Ministry of Health, Labour and Welfare of Japan; Program for Promotion of Fundamental Studies in Health Science from the National Institute of Biomedical Innovation; a grant provided by the Ichiro Kanehara Foundation; Ground-based Research Announcement for Space Utilization promoted by the Japan Space Forum; and Industrial Technology Research Grant Program 03A47075 from the New Energy and Industrial Technology Development Organization of Japan.

REFERENCES

1. **Akiyama T, Yamazaki T.** Norepinephrine release from cardiac sympathetic nerve endings in the in vivo ischemic region. *J Cardiovasc Pharmacol* 34: S11–S14, 1999.

2. **Akiyama T, Yamazaki T, Ninomiya I.** In vivo monitoring of myocardial interstitial norepinephrine by dialysis technique. *Am J Physiol Heart Circ Physiol* 261: H1643–H1647, 1991.
3. **Akiyama T, Yamazaki T, Ninomiya I.** In vivo detection of endogenous acetylcholine release in cat ventricles. *Am J Physiol Heart Circ Physiol* 266: H854–H860, 1994.
4. **Chernow B, Lake CR, Zaritsky A, Finton CK, Casey L, Rainey TG, Fletcher JR.** Sympathetic nervous system "switch off" with severe hypothermia. *Crit Care Med* 11: 677–680, 1983.
5. **Damsma G, Fibiger HC.** The effects of anaesthesia and hypothermia on interstitial concentrations of acetylcholine and choline in rat striatum. *Life Sci* 48: 2469–2474, 1991.
6. **Duncker DJ, Klassen CL, Ishibashi Y, Herrlinger SH, Pavek T, Bache R.** Effect of temperature on myocardial infarction in swine. *Am J Physiol Heart Circ Physiol* 270: H1189–H1199, 1996.
7. **Genth K, Hofmann M, Hofmann M, Schaper W.** The effect of β-adrenergic blockade on infarct size following experimental coronary occlusion. *Basic Res Cardiol* 76: 144–151, 1981.
8. **Gerevich Z, Tretter L, Adam-Vizi V, Baranyi M, Kiss JP, Zelles T, Vizi ES.** Analysis of high intracellular [Na^+]-induced release of [^{3}H]noradrenaline in rat hippocampal slices. *Neuroscience* 104: 761–768, 2001.
9. **Hale SL, Kloner RA.** Myocardial temperature in acute myocardial infarction: protection with mild regional hypothermia. *Am J Physiol Heart Circ Physiol* 273: H220–H227, 1997.
10. **Jang IK, Van de Werf F, Vanhaecke J, De Geest H.** Coronary reperfusion by thrombolysis and early beta-adrenergic blockade in acute experimental myocardial infarction. *J Am Coll Cardiol* 14: 1816–1823, 1989.
11. **Kakinuma Y, Ando M, Kuwabara M, Katare RG, Okudela K, Kobayashi M, Sato T.** Acetylcholine from vagal stimulation protects cardiomyocytes against ischemia and hypoxia involving additive nonhypoxic induction of HIF-1α. *FEBS Lett* 579: 2111–2118, 2005.
12. **Kao LS, Westhead EW.** Temperature dependence of catecholamine secretion from cultured bovine chromaffin cells. *J Neurochem* 43: 590–592, 1984.
13. **Kawada T, Yamazaki T, Akiyama T, Sato T, Shishido T, Inagaki M, Takaki H, Sugimachi M, Sunagawa K.** Differential acetylcholine release mechanisms in the ischemic and non-ischemic myocardium. *J Mol Cell Cardiol* 32: 405–414, 2000.
14. **Kawada T, Yamazaki T, Akiyama T, Shishido T, Inagaki M, Uemura K, Miyamoto T, Sugimachi M, Takaki H, Sunagawa K.** In vivo assessment of acetylcholine-releasing function at cardiac vagal nerve terminals. *Am J Physiol Heart Circ Physiol* 281: H139–H145, 2001.
15. **Kitagawa H, Akiyama T, Yamazaki T.** Effects of moderate hypothermia on in situ cardiac sympathetic nerve endings. *Neurochem Int* 40: 235–242, 2002.
16. **Kitagawa H, Yamazaki T, Akiyama T, Mori H, Sunagawa K.** Effects of moderate hypothermia on norepinephrine release evoked by ouabain, tyramine and cyanide. *J Cardiovasc Pharmacol* 41: S111–S114, 2003.
17. **Ku DD, Lucchesi BR.** Effects of dimethyl propranolol (UM-272; SC-27761) on myocardial ischemic injury in the canine heart after temporary coronary artery occlusion. *Circulation* 57: 541–548, 1978.
18. **Kurz T, Richardt G, Hagl S, Seyfarth M, Schömig A.** Two different mechanisms of noradrenaline release during normoxia and simulated ischemia in human cardiac tissue. *J Mol Cell Cardiol* 27: 1161–1172, 1995.
19. **Lameris TW, de Zeeuw S, Alberts G, Boomsma F, Duncker DJ, Verdouw PD, Veld AJ, van den Meiracker AH.** Time course and mechanism of myocardial catecholamine release during transient ischemia in vivo. *Circulation* 101: 2645–2650, 2000.
20. **Lameris TW, de Zeeuw S, Duncker DJ, Alberts G, Boomsma F, Verdouw PD, van den Meiracker AH.** Exogenous angiotensin II does not facilitate norepinephrine release in the heart. *Hypertension* 40: 491–497, 2002.
21. **Maxwell MP, Hearse DJ, Yellon DM.** Species variation in the coronary collateral circulation during regional myocardial ischaemia: a critical determinant of the rate of evolution and extent of myocardial infarction. *Cardiovasc Res* 21: 737–746, 1987.
22. **Rona G.** Catecholamine cardiotoxicity. *J Mol Cell Cardiol* 17: 291–306, 1985.
23. **Schwartz JH.** Neurotransmitters. In: *Principles of Neural Science* (4th Ed.), edited by Kandel ER, Schwartz JH, Jessell TM. New York: McGraw-Hill, 2000, p. 280–297.
24. **Schömig A, Kurz T, Richardt G, Schömig E.** Neuronal sodium homeostasis and axoplasmic amine concentration determine calcium-independent noradrenaline release in normoxic and ischemic rat heart. *Circ Res* 63: 214–226, 1988.
25. **Simkhovich BZ, Hale SL, Kloner RA.** Metabolic mechanism by which mild regional hypothermia preserves ischemic tissue. *J Cardiovasc Pharmacol Ther* 9: 83–90, 2004.
26. **Toombs CF, Wiltse AL, Shebuski RJ.** Ischemic preconditioning fails to limit infarct size in reserpinized rabbit myocardium. Implication of norepinephrine release in the preconditioning effect. *Circulation* 88: 2351–2358, 1993.
27. **Torr S, Drake-Holland AJ, Main M, Hynd J, Isted K, Noble MIM.** Effects on infarct size of reperfusion and pretreatment with β-blockade and calcium antagonists. *Basic Res Cardiol* 84: 564–582, 1989.
28. **Van den Doel MA, Gho BC, Duval SY, Schoemaker RG, Duncker DJ, Verdouw PD.** Hypothermia extends the cardioprotection by ischaemic preconditioning to coronary artery occlusions of longer duration. *Cardiovasc Res* 37: 76–81, 1998.
29. **Vander Heide RS, Schwartz LM, Jennings RB, Reimer KA.** Effect of catecholamine depletion on myocardial infarct size in dogs: role of catecholamines in ischemic preconditioning. *Cardiovasc Res* 30: 656–662, 1995.
30. **Vizi ES.** Different temperature dependence of carrier-mediated (cytoplasmic) and stimulus-evoked (exocytotic) release of transmitter: a simple method to separate the two types of release. *Neurochem Int* 33: 359–366, 1998.
31. **Yamazaki T, Akiyama T, Kitagawa H, Takauchi Y, Kawada T, Sunagawa K.** A new, concise dialysis approach to assessment of cardiac sympathetic nerve terminal abnormalities. *Am J Physiol Heart Circ Physiol* 272: H1182–H1187, 1997.
32. **Zheng F, Kidd C, Bowser-Riley F.** Effects of moderate hypothermia on baroreflex and pulmonary chemoreflex heart rate response in decerebrate ferrets. *Exp Physiol* 81: 409–420, 1996.

Am J Physiol Heart Circ Physiol 292: H921–H927, 2007.
First published September 29, 2006; doi:10.1152/ajpheart.00019.2006.

Evaluation of transmural distribution of viable muscle by myocardial strain profile and dobutamine stress echocardiography

Takeshi Maruo,[1] Satoshi Nakatani,[1] Yintie Jin,[2] Kazunori Uemura,[2] Masaru Sugimachi,[2] Hatsue Ueda-Ishibashi,[3] Masafumi Kitakaze,[1] Tohru Ohe,[4] Kenji Sunagawa,[2] and Kunio Miyatake[1]

Departments of [1]Cardiology and [3]Pathology, National Cardiovascular Center, and [2]Department of Cardiovascular Dynamics, National Cardiovascular Center Research Institute, Osaka, Japan; and [4]Department of Cardiovascular Medicine, Okayama University Graduate School of Medicine, Okayama, Japan

Submitted 5 January 2006; accepted in final form 27 September 2006

Maruo T, Nakatani S, Jin Y, Uemura K, Sugimachi M, Ueda-Ishibashi H, Kitakaze M, Ohe T, Sunagawa K, Miyatake K. Evaluation of transmural distribution of viable muscle by myocardial strain profile and dobutamine stress echocardiography. *Am J Physiol Heart Circ Physiol* 292: H921–H927, 2007. First published September 29, 2006; doi:10.1152/ajpheart.00019.2006.—Transmural distribution of viable myocardium in the ischemic myocardium has not been quantified and fully elucidated. To address this issue, we evaluated transmural myocardial strain profile (TMSP) in dogs with myocardial infarction using a newly developed tissue strain imaging. TMSP was obtained from the posterior wall at the epicardial left ventricular short-axis view in 13 anesthetized open-chest dogs. After control measurements, the left circumflex coronary artery was occluded for 90 min to induce subendocardial infarction (SMI). Subsequently, latex microbeads (90 μm) were injected in the same artery to create transmural infarction (TMI). In each stage, measurements were done before and after dobutamine challenge (10 $\mu g \cdot kg^{-1} \cdot min^{-1}$ for 10 min) to estimate transmural myocardial viability. Strain in the subendocardium in the control stage increased by dobutamine (from 53.6 ± 17.1 to 73.3 ± 21.8%, $P < 0.001$), whereas that in SMI and TMI stages was almost zero at baseline and did not increase significantly by dobutamine [from 0.8 ± 8.8 to 1.3 ± 7.0%, P = not significant (NS) for SMI, from −3.9 ± 5.6 to −1.9 ± 6.0%, P = NS for TMI]. Strain in the subepicardium increased by dobutamine in the control stage (from 23.9 ± 6.1 to 26.3 ± 6.4%, $P < 0.05$) and in the SMI stage (from 12.4 ± 7.3 to 27.1 ± 8.8%, $P < 0.005$), whereas that in the TMI stage did not change (from −1.0 ± 7.8 to −0.7 ± 8.3%, P = NS). In SMI, the subendocardial contraction was lost, but the subepicardium showed a significant increase in contraction with dobutamine. However, in TMI, even the subepicardial increase was not seen. Assessment of transmural strain profile using tissue strain imaging was a new and useful method to estimate transmural distribution of the viable myocardium in myocardial infarction.

myocardial infarction; strain; viability; echocardiography

IT IS WELL KNOWN that myocardial contraction has transmural heterogeneity. Several experimental studies confirmed that the subendocardium contributes greater to overall myocardial thickening than the subepicardium (6, 25). On the other hand, when a reduction of coronary blood flow occurs, a severe reduction of perfusion and kinesis occurs in the subendocardium, but only a trivial reduction can be detected in the subepicardium (5, 31). After a long period of ischemia, myocardial necrosis progresses from the endocardium to the epicardium (8, 13).

Myocardial strain reflects regional myocardial function. With the recent advancement of tissue Doppler echocardiography, myocardial strain can be obtained noninvasively (3, 33) and has been reported to be useful to quantify regional myocardial systolic function in ischemic heart disease (9, 11, 24, 29, 36). The recently developed myocardial strain imaging system provides us myocardial strain in each wall layer and shows its distribution in a form of transmural myocardial strain profile (TMSP; see Ref. 1). Thus combination of TMSP and dobutamine stress echocardiography (DSE), which has been used for the assessment of myocardial viability (18), is expected to demonstrate transmural distribution of viability. There have been no methods to visualize distribution of myocardial viability over the ventricular wall in myocardial infarction, and such method would provide important information in the clinical situation.

In the present study, to assess the transmural extent of myocardial infarction, we investigated TMSP in subendocardial and transmural myocardial infarction dog models and quantified the transmural heterogeneity of myocardial viability using myocardial strain imaging with DSE.

MATERIALS AND METHODS

Experimental subjects and settings. We used 13 mongrel dogs (weighing 27.3 ± 2.2 kg). After induction with intravenous pentobarbital sodium (25 mg/kg body wt), they were anesthetized with 2% isoflurane with oxygen. A median sternotomy was performed, the pericardium was split from apex to base, and, after the instrumentation, the edges of the pericardial incision were loosely resutured. A 5-Fr. micromanometer-tipped catheter (model MPC-500; Millar Instruments, Houston, TX) was positioned in the left ventricle through the apex to obtain peak systolic left ventricular pressure and peak positive and negative dP/dt. Electrocardiogram (ECG) was monitored from limb leads. Left ventricular pressure signals and ECG were digitized online. The care and use of animals was in strict accordance with the guiding principles of the American Physiological Society, and the experimental protocol was approved by the National Cardiovascular Center Committees on Animal Experiments.

Experimental protocol. A 6-Fr. sheath was placed in the right femoral artery, and an angioplasty balloon catheter was positioned in the proximal segment of the left circumflex coronary artery by the standard catheterization technique. DSE (dobutamine infusion at 10 $\mu g \cdot kg^{-1} \cdot min^{-1}$ for 10 min) was used to assess myocardial viability. At the control stage, echocardiographic and hemodynamic measurements were done before and after DSE. A subendocardial myocardial infarction was created by inflating the balloon for 90 min

Address for reprint requests and other correspondence: S. Nakatani, Dept. of Cardiology, National Cardiovascular Center, 5-7-1, Fujishiro-dai, Suita, Osaka 565-8565, Japan (e-mail: nakatas@hsp.ncvc.go.jp).

The costs of publication of this article were defrayed in part by the payment of page charges. The article must therefore be hereby marked "*advertisement*" in accordance with 18 U.S.C. Section 1734 solely to indicate this fact.

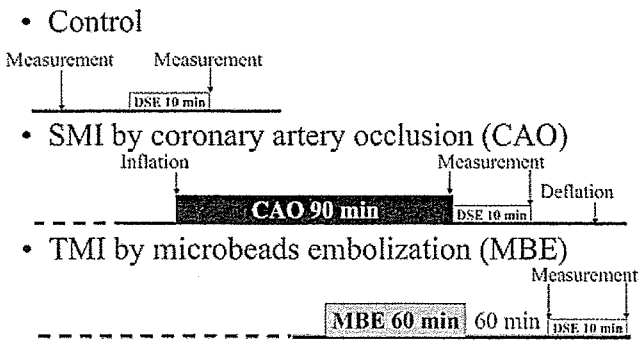

Fig. 1. Experimental protocol. DSE, dobutamine stress echocardiography; SMI, subendocardial myocardial infarction; TMI, transmural myocardial infarction.

(SMI stage; see Refs. 8 and 10), and DSE was performed during balloon inflation. After balloon deflation, 200–300 mg of latex microbeads (diameter 90 μm) were slowly injected in the same artery in 60 min to create a transmural myocardial infarction (TMI stage; see Refs. 7, 12, 15). At the TMI stage, DSE was performed 60 min after microbead embolization to complete myocardial infarction and to avoid ventricular instability to dobutamine challenge, and measurements were done before and after DSE (Fig. 1).

Ultrasound data acquisition. A commercially available ultrasound scanner (PowerVision 8000 3.5-MHz transducer; Toshiba, Tokyo, Japan) was used to obtain the epicardial left ventricular short-axis images at the level of basal and midventricle by tissue Doppler imaging. Recordings were stored in the form of digital loops of two cardiac cycles with 96–102 frames/s for subsequent analysis (33).

Tissue strain imaging. Strain is defined by the equation below and expresses the deformation of an object,

$$\text{Strain} = (L - L_0)/L_0$$

where L_0 is the length of an object before deformation and L is that after or during deformation. In echocardiography, L_0 is usually a muscle length at end diastole, and myocardial strain is used to express the deformation of local myocardial segments (4, 33).

In the present study, myocardial radial strain image was obtained from off-line analysis by using a research software TDI-Q (Toshiba; see Ref. 3). To obtain a strain image, TDI-Q software first calculates the myocardial displacement of all pixels of tissue by integrating myocardial velocity over a certain period. Because the frame rate was 96–102 frames/s, the step size for integration was 9.8–10.4 ms. Next, strain is obtained by evaluating the change of distance between pairs of two points defined on all pixels on the image by utilizing the displacement values. The distance of all two-pixel pairs at the initial time frame is equivalent to "L_0" on the above equation and set at 3 mm in this study (17). The initial time frame is set at end diastole to evaluate contraction; in other words "deformation" of the myocardium occurring in systole.

To measure local strain accurately, it is indispensable to obtain local velocity accurately. Therefore, the present myocardial strain imaging system has adopted tissue Doppler tracking and angle-correction techniques. Tissue Doppler tracking is an automatic motion tracking technique based on tissue Doppler information (30). By integrating a velocity of an indexed point on the ventricular wall known from tissue Doppler imaging, we can obtain myocardial displacement and predict the point where that point moves next. By repeating this procedure, the system can automatically track the motion of the point. With this technique, the influence of myocardial translation can be neglected. The angle-correction technique enables us to partly overcome the Doppler incident angle dependency that is inherent in Doppler echocardiography, as previous reports described (3, 26, 32). To correct the Doppler incident angle, a contraction center is set at the center of the left ventricular cavity at end systole in the left ventricular short-axis view. Next, the software automatically calculates the tissue velocity toward the contraction center (V_{motion}) by dividing the velocity toward a transducer (V_{beam}) by the cosine of the angle (θ) between the Doppler beam and the direction to the contraction center as follows:

$$V_{\text{motion}} = V_{\text{beam}}/\cos\theta$$

With the use of these two techniques, the research software TDI-Q automatically cancelled the effect of myocardial translation and angle dependency, accurately providing myocardial velocity, displacement, and strain (3). In the previously described experiments, the displacement data obtained by this method correlated with true displacement ($r = 0.99$, $P < 0.0001$; see Ref. 26).

Myocardial radial strain distribution over the myocardium is obtained as M-mode color-coded images, and the profile of distribution (TMSP) at end systole is shown as in Fig. 2. Bright color indicates high strain, and dark color indicates low strain. We obtained TMSP at basal and midinferolateral walls at end systole. We divided the myocardium into subendocardial and subepicardial half-layers by the midpoint of the myocardium at end systole. Mean strain values in the subendocardial half-layer and in the subepicardial half-layer were calculated by averaging strain values over each layer.

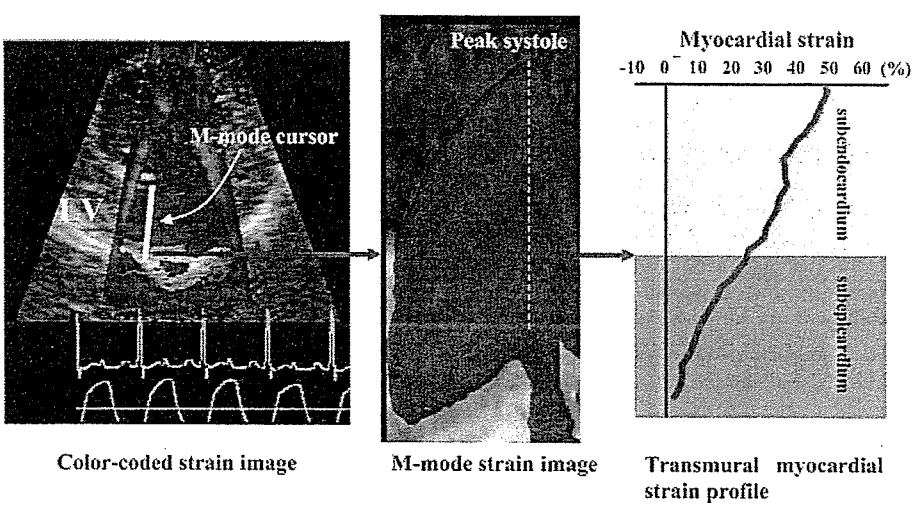

Fig. 2. Color-coded strain imaging, M-mode strain imaging, and transmural myocardial strain profile imaging in the control stage. *Left*: myocardial strain imaging of the left ventricular short axis at end systole. Red color means myocardial thickening. A white bar indicates an M-mode cursor. *Middle*: color-coded M-mode myocardial strain imaging obtained at the left ventricular posterior wall. The subendocardium is brighter than the subepicardium, indicating that the subendocardium contracts more vigorously. *Right*: transmural strain profile at end systole. The strain was highest at the subendocardium and lowest at the subepicardium, and the transmural strain showed a linear profile. LV, left ventricular wall.

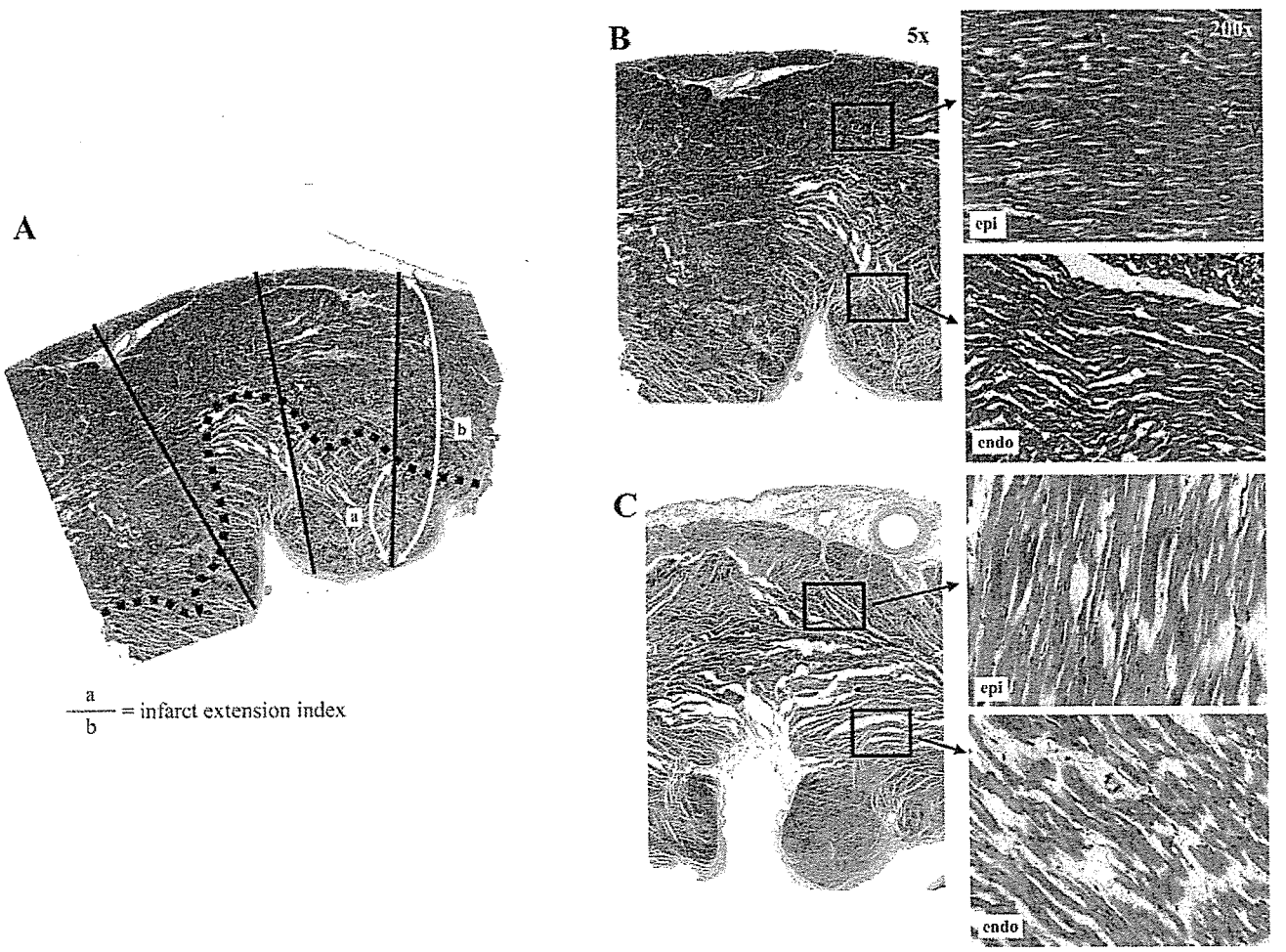

Fig. 3. *A*: determination of infarct extension index. Dotted line indicates the external limit of the infarcted zone. Examples of myocardial specimens taken after the SMI stage (*B*) and the TMI stage (*C*) stained by Masson's trichrome staining. In the SMI specimen, myocardial infarct was found only in the subendocardial layer, whereas acute ischemic changes such as wavy change or coagulation necrosis were recognized in both subendocardial and subepicardial layers in the TMI specimen. endo, Subendocardial layer; epi, subepicardial layer.

Histopathological studies. Establishment of subendocardial and transmural infarction by these techniques has been confirmed in our preliminary study and other previous studies (8, 10). We assessed the degree of extension of myocardial infarct also in the present study. At the end of the SMI stage in four dogs and the TMI stage in seven dogs, the heart was excised and cut into five to seven equally distant short-axis slices. Each slice was stained with hematoxylin-eosin and Masson's trichrome (Fig. 3). A pathologist who was blind to the experimental data examined the hearts histologically and measured the degree of infarct extension at the basal and midinferolateral walls, as previously reported (2). On each enlarged photomicrograph of the hearts, three to five transmural radii in the infarcted area were traced perpendicular to the endocardial and epicardial borders. The distance from the endocardial border to the external limit of the infarcted zone was measured and was expressed as a percentage of the distance between the endocardial and epicardial borders as an index of infarct extension, 100% being fully transmural and 0% being no infarction.

Table 1. *Hemodynamic parameters in control, SMI, and TMI stages*

	Baseline			DSE		
	Control (n = 13)	SMI (n = 11)	TMI (n = 7)	Control	SMI	TMI
HR, beats/min	133±17	128±27	129±27	149±22	134±27	150±19
LVP, mmHg	123±10*†	108±24	92±21	136±11†	132±28†	112±20
+dP/dt, mmHg/s	2,169±484*†‡	1,577±347*†	1,207±279*	4,021±979†‡	3,231±844†	2,478±1,138
−dP/dt, mmHg/s	−2,531±408*†	−1,824±606*†	−1,164±465*	−3,188±650†	−2,724±892	−2,104±526

Data are presented as means ± SD; n, no. of dogs. DSE, dobutamine stress echocardiography; SMI, subendocardial myocardial infarction; TMI, transmural myocardial infarction; HR, heart rate; LVP, peak systolic left ventricular pressure; +dP/dt, peak positive dP/dt; −dP/dt, peak negative dP/dt. $P < 0.05$ vs. DSE values (*), vs. SMI values (‡), and vs. TMI values (†).